

# Death from drought in tropical forests is triggered by hydraulics not carbon starvation

L. Rowland<sup>1</sup>, A. C. L. da Costa<sup>2</sup>, D. R. Galbraith<sup>3</sup>, R. S. Oliveira<sup>4</sup>, O. J. Binks<sup>1</sup>, A. A. R. Oliveira<sup>2</sup>, A. M. Pullen<sup>5</sup>, C. E. Doughty<sup>6</sup>, D. B. Metcalfe<sup>7</sup>, S. S. Vasconcelos<sup>8</sup>, L. V. Ferreira<sup>9</sup>, Y. Malhi<sup>6</sup>, J. Grace<sup>1</sup>, M. Mencuccini<sup>1,10</sup> & P. Meir<sup>1,11</sup>

**Drought threatens tropical rainforests over seasonal to decadal timescales<sup>1–4</sup>, but the drivers of tree mortality following drought remain poorly understood<sup>5,6</sup>. It has been suggested that reduced availability of non-structural carbohydrates (NSC) critically increases mortality risk through insufficient carbon supply to metabolism ('carbon starvation')<sup>7,8</sup>. However, little is known about how NSC stores are affected by drought, especially over the long term, and whether they are more important than hydraulic processes in determining drought-induced mortality. Using data from the world's longest-running experimental drought study in tropical rainforest (in the Brazilian Amazon), we test whether carbon starvation or deterioration of the water-conducting pathways from soil to leaf trigger tree mortality. Biomass loss from mortality in the experimentally droughted forest increased substantially after >10 years of reduced soil moisture availability. The mortality signal was dominated by the death of large trees, which were at a much greater risk of hydraulic deterioration than smaller trees. However, we find no evidence that the droughted trees suffered carbon starvation, as their NSC concentrations were similar to those of non-droughted trees, and growth rates did not decline in either living or dying trees. Our results indicate that hydraulics, rather than carbon starvation, triggers tree death from drought in tropical rainforest.**

Drought-response observations from both field-scale experiments and natural droughts have demonstrated increased mortality over the short-term (1–3 years), with notably higher vulnerability for some taxa, and for larger trees<sup>6,9,10</sup>. After several years of drought, recovering growth rates in smaller trees, dbh (diameter at breast height) <40 cm, and reduced mortality have been recorded at different locations<sup>6,11,12</sup>. However, the long-term (>10 year) sensitivity of tropical forests to predicted prolonged and repeated water deficit<sup>1–3</sup> and the physiological mechanisms influencing this are poorly understood. Through-fall exclusion (TFE) studies, that create soil moisture deficit by the exclusion of a fraction of incoming rainfall, provide the only current means to assess the long-term response in mechanistic detail<sup>5,13</sup>.

Trees experiencing drought stress are thought to die from direct physiological failure and/or from injury and biotic attack associated with a decline in physiological vigour<sup>14</sup>. A global effort to identify the relevant physiological mechanisms triggering death and thus to improve predictions of forest tree mortality has focused on the twin possibilities of: (1) failure to supply sufficient carbon substrate to metabolism following drought-related reductions in photosynthesis and increased use of NSC, theoretically leading to carbon starvation; and (2) deterioration of the water-conducting xylem tissue, causing a rapid or gradual failure of key dependent processes (for example, gas exchange, photosynthesis, phloem transport), and potentially leading to tissue desiccation<sup>14,15</sup>, ultimately leading to mortality. Despite recent

intensive research, it is unclear how important these two mechanisms are in different biomes and how, or whether, to model them<sup>16</sup>.

Since 2002 a 50% TFE treatment has been implemented at a 1 ha-scale drought experiment in old-growth forest at Caxiuanã National Forest Reserve, Pará State, Brazil<sup>6,12</sup>, to simulate maximum possible rainfall reductions predicted to occur in parts of Amazonia by 2100 (ref. 1). Mortality surveys, recruitment and growth rates of all trees  $\geq 10$  cm dbh, have been monitored through the experimental period (see Methods). Recently, seasonal data on NSC concentrations were measured on leaves, branches and stems of 41 trees (20 trees on the control, 21 trees on the TFE) of the most common genera in the experiment (Extended Data Table 1). Xylem vulnerability curves were also performed on the branches of these trees (see Methods). Here, we synthesize these data to test whether long-term soil moisture deficit alters NSC storage and use in tropical rainforest trees, and if this, or hydraulic processes, are most strongly associated with increased mortality rates.

By 2014, following 13 years of the TFE treatment, cumulative biomass loss through mortality was  $41.0 \pm 2.7\%$  relative to pre-treatment values (Fig. 1a), and the rate of loss had increased substantially since the previous reported value of  $17.2 \pm 0.8\%$ , after 7 years of TFE<sup>6</sup>. Accelerating biomass loss and failure to recover substantially, or to reach a new equilibrium<sup>13</sup>, has led to a committed flux to the atmosphere from decomposing necromass of  $101.9 \pm 19.1$  Mg C ha<sup>-1</sup> (Fig. 1a). This biomass loss has been driven by elevated mortality in the largest trees (Fig. 1b), as previously observed over shorter timescales<sup>6</sup>, and has created a canopy that has had a persistently lower average leaf area index during 2010–2014 ( $12.0 \pm 1.2\%$  lower; Extended Data Fig. 1).

Remarkably, individual tree growth rates for the four years before death showed no significant reduction in either the TFE or control plots (Fig. 2a), indicating that growth is prioritised to the point of death irrespective of the soil moisture deficit treatment. From 2008, tree growth in every wet season (January–June) on the TFE treatment relative to the control was significantly elevated ( $P < 0.05$ ) in the small and medium trees (up to  $4.6 \pm 0.2$  times higher in small trees, and  $2.9 \pm 0.2$  times higher in medium trees), and maintained in the largest trees (10–20 cm, 20–40 cm and >40 cm dbh, respectively; Fig. 2b–d). Elevated wet season growth occurred despite 0.1–0.9 MPa reduction in average soil water potential ( $\Psi_s$ ) at depths of 0–4 m on the TFE and a loss of seasonality in  $\Psi_s$  (Extended Data Fig. 2). Increased growth in the small trees occurred from 2008 onwards, following earlier substantial mortality of large trees (Fig. 1), which generated canopy gaps. Increased light availability to smaller trees and, presumably, reduced below-ground competition for water and nutrients, allowed competitive release of trees on the TFE<sup>8</sup>, and elevated growth rates. Competitive release on the TFE implies that, following 13 years of drought-stress, photosynthetic production is sufficient not only to maintain growth in the largest trees (Fig. 2d), but to increase growth

<sup>1</sup>School of GeoSciences, University of Edinburgh, Edinburgh EH9 3FF, UK. <sup>2</sup>Centro de Geociências, Universidade Federal do Pará, Belém 66075-110, Brazil. <sup>3</sup>School of Geography, University of Leeds, Leeds LS2 9JT, UK. <sup>4</sup>Instituto de Biologia, UNICAMP, Campinas 13.083-970, Brazil. <sup>5</sup>The University of Cambridge, Cambridge CB2 1TN, UK. <sup>6</sup>Environmental Change Institute, The University of Oxford, Oxford OX1 3QY, UK. <sup>7</sup>Department of Physical Geography and Ecosystem Science, Lund University, Lund S-223 62, Sweden. <sup>8</sup>EMBRAPA Amazônia Oriental, Belém 66095-903, Brazil. <sup>9</sup>Museu Paraense Emílio Goeldi, Belém 66077-830, Brazil. <sup>10</sup>CREA at CREA, 08193 Cerdanyola del Vallés, Spain. <sup>11</sup>Research School of Biology, Australian National University, Canberra, Australian Capital Territory 2601, Australia.

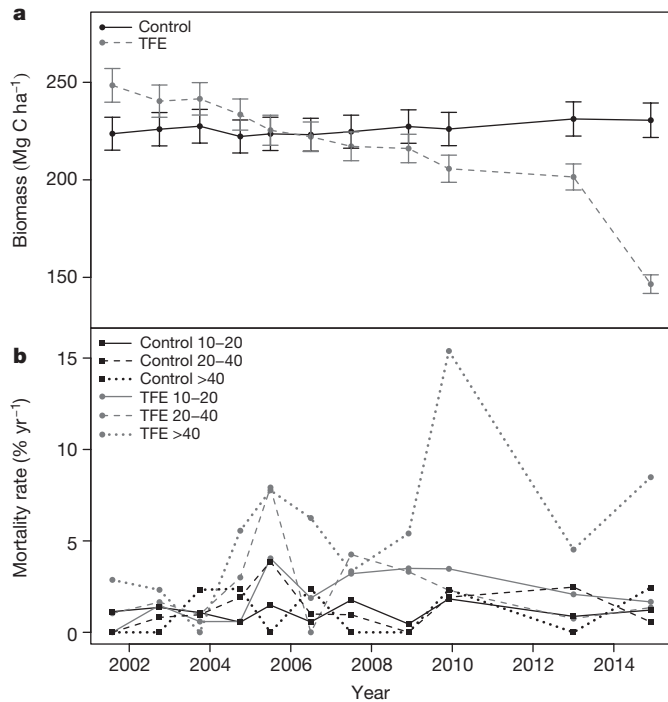


**Figure 1 | Changes in biomass and mortality rates.** **a**, Biomass on the control and TFE plot from 2001–2014 ( $\text{Mg C ha}^{-1} \text{ yr}^{-1}$ ). Error bars show the s.e.m. calculated from 12 estimates of biomass for trees on the control plot ( $n = 369$ ) and TFE ( $n = 358$ ), accounting for uncertainty in wood density and allometric equations (see Methods). **b**, Mortality rate (% stems per year) for trees on the control plot (black) and TFE (grey) separated for trees of 10–20 cm dbh (control  $n = 164$ –193, TFE  $n = 132$ –174, with range showing 2001–2014 maximum and minimum  $n$ ), 20–40 cm (control  $n = 97$ –105, TFE  $n = 81$ –104), dbh and >40 cm (control  $n = 41$ –45, TFE  $n = 17$ –37). The genus and date of death for each tree used in the mortality rate calculations is shown in Extended Data Table 3.

in trees <40 cm dbh (Fig. 2b, c). This response would not be possible if the majority of trees were severely carbon limited, unless very considerable long-term (or renewed) carbon resources were being drawn upon.

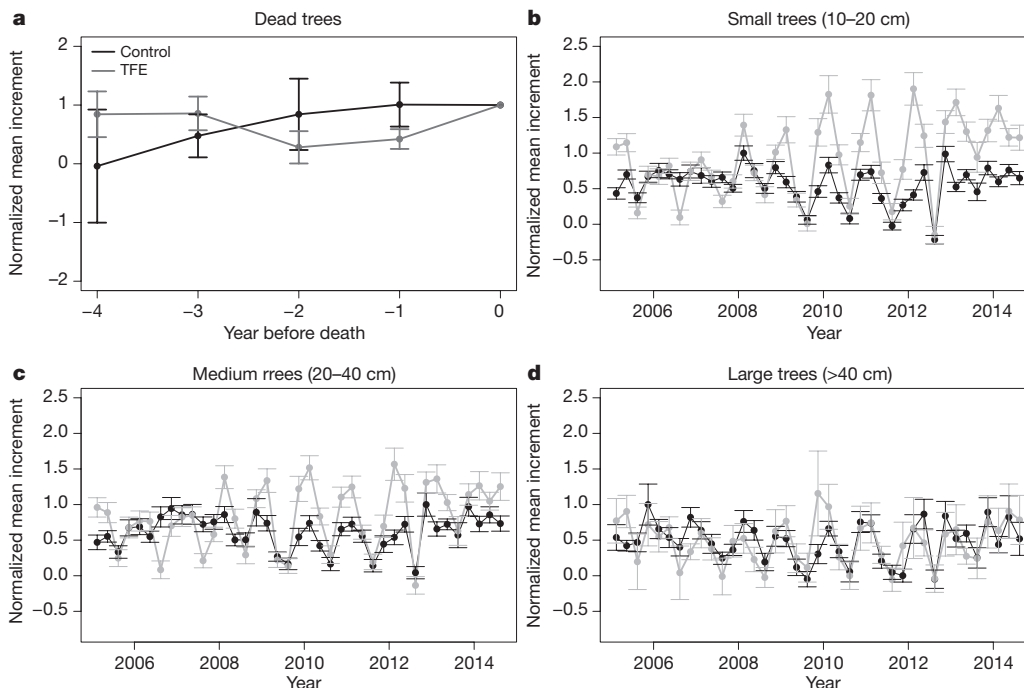


**Figure 2 | Tree growth of living and dead trees.** **a**, Average annual stem increment in the 4 years before death for all trees which died on the control ( $n = 35$ ) and TFE ( $n = 60$ ) from 2005 onwards. Growth rates are normalized by the growth in year 0, the year in which the tree died. **b–d**, Stem increment for small (**a**, 10–20 cm dbh,  $n = 153$ ,  $n = 116$ ), medium (**b**, 20–40 cm dbh,  $n = 73$ ,  $n = 78$ ) and large (**c**, >40 cm dbh,  $n = 18$ ,  $n = 8$ ) trees on the control and TFE plot respectively from 2005 to 2014. Values for **b–d** are normalized by the maximum increment on the control plot. Error bars show the s.e.m.

Prioritization of growth under drought in the TFE is consistent with recent observations following short-term drought in Amazonia<sup>7</sup>. However, the maintenance of NSC concentrations in the TFE treatment suggests that the prioritisation of growth during drought does not occur at the expense of depleted carbon stores, as previously hypothesized<sup>7</sup>. Neither the concentrations of soluble sugar (carbon immediately available to metabolism) nor starch (stored carbon which can be converted to sugars) were significantly depleted in stem, leaf and branch tissue from the TFE, relative to control (Fig. 3). The seasonal changes in both sugar and starch concentrations, which varied by 50–90%, were much larger than any differences associated with the TFE treatment (Fig. 3). Despite 13 years of severely reduced soil moisture availability, the seasonal cycle and use of NSCs was unaltered, implying that the sampled trees did not draw significantly upon their NSC reserves to buffer against the long-term effects of soil moisture deficit. Large changes in carbon allocation from roots and leaves to maintain stem growth during drought<sup>17</sup> have not been reported on the TFE<sup>12</sup>. Similarly, no drought-induced reductions in photosynthetic capacity occurred on the TFE<sup>18</sup>, although how total canopy productivity is affected remains uncertain. Considering this and additional evidence of no increase in herbivore attack on the TFE (Extended Data Fig. 3), our results suggest progressive carbon starvation and biotic foliar consumption are not important drivers of the mortality patterns observed in the TFE forest following extended severe soil moisture deficit (>10 years).

Deterioration of the water transport system in the xylem tissues following drought can also lead to death<sup>17,19</sup>. The vulnerability of the xylem to drought is described by a vulnerability curve<sup>20</sup>, which relates water potential in xylem conduits to loss of hydraulic conductivity because of occlusions by gas emboli. The water potential at which 50% loss of xylem conductivity occurs ( $P_{50}$ , MPa) is a commonly used index of embolism resistance<sup>20</sup>. We determined xylem  $P_{50}$  for the trees on the control and TFE plots, with tree dbh ranging from 15 to 48 cm. A highly significant decrease in  $P_{50}$  with dbh was found across TFE and control (Extended Data Table 2,  $P < 0.01$ ). As dbh increased from 15 to 48 cm there was a  $1.3 \pm 0.2$  MPa reduction in the  $P_{50}$  value, with significant genus-to-genus differences (Fig. 4). Leaf water potential ( $\Psi_l$ ) could only be measured during limited sampling campaigns (2–3 days) that were characterized by low vapour pressure deficit (VPD, 54–59% of peak dry season values) and unseasonal rainfall in the preceding days. Differences between treatment and control  $\Psi_l$  were not detected. Mean midday  $\Psi_l$  recorded across

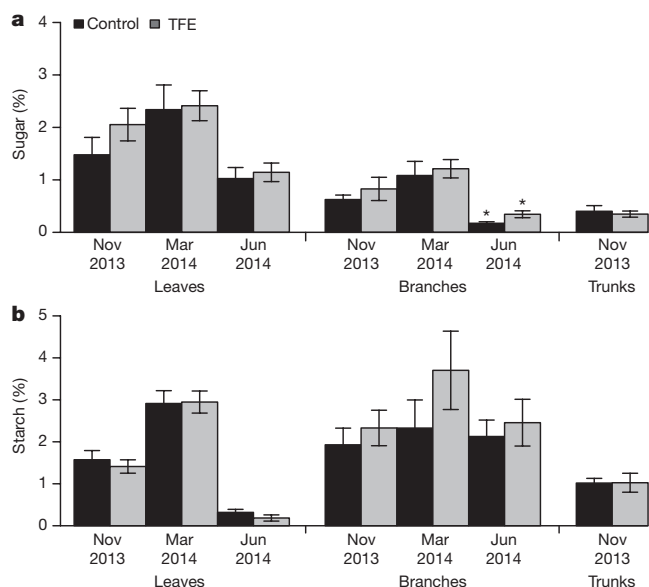


**Figure 3 | Leaf, branch and stem NSC concentrations.** **a, b,** Percentage of soluble sugars (**a**) and starch (**b**) in biomass of leaves, branches and stems, in the late dry season (November 2013), mid wet season (March 2014) and in the wet-to-dry transition (June 2014). Each value for leaves, branches or stems represents an average of samples taken from  $n = 20$  trees on the control, and  $n = 21$  trees on the TFE. TFE Error bars show s.e.m. and \* indicates a significant difference at  $P < 0.05$  using the Wilcoxon test. June 2014 has significantly elevated sugar values on the TFE plot; however, the absolute values for sugar concentration are very low, and the absolute differences are very small.

all the trees together with the vulnerability curves determined for each genus were used to predict the percentage loss of xylem conductivity (PLC) with dbh. Values of PLC at mean  $\Psi_1$  increased with dbh, with the largest diameter trees predicted to have reductions in conductive capacity of about 80% in some genera, indicating significant vulnerability to hydraulic deterioration (inset of Fig. 4).

Given no evidence of carbon starvation and similar  $\Psi_1$  across plots in the sample dates, why did many more trees die in TFE than control? The lack of treatment differences in  $\Psi_1$  contrasts starkly with the long-term records of lower  $\Psi_s$  (Extended Data Fig. 2). The lack of difference

in midday  $\Psi_1$  could have been caused by sampling constraints or by isohydric behaviour. We found evidence of non-isohydric behaviour in our diurnal  $\Psi_1$  measurements (Extended Data Fig. 4), with overall strong linear declines in  $\Psi_1$  observed with increasing VPD on the control ( $R^2 = 0.18$ ,  $P < 0.01$ ) and in particular on the TFE ( $R^2 = 0.33$ ,  $P < 0.01$ ). Consequently, limited sampling is the most likely cause of equal  $\Psi_1$  between the two plots, with TFE trees likely to be having more negative  $\Psi_1$  and lower hydraulic conductance during VPD maxima in the dry season. Reduced carbon uptake because of stomatal closure in some TFE trees is possible<sup>21</sup>, but is unlikely to have caused carbon starvation considering that growth rates were maintained or elevated on the TFE (Fig. 2) and that radial growth should decline before photosynthesis in drought conditions<sup>22</sup>. Even with an isohydric response, trees on the TFE would still be likely to suffer greater hydraulic deterioration caused by greater PLC in the roots and main stem. Strongly reduced  $\Psi_s$  on the TFE (Extended Data Fig. 2) and significant hydraulic vulnerability of the tall trees are consistent with the hypothesis of hydraulic deterioration as the most likely trigger of greater mortality, particularly in the largest trees, as observed. Why the xylem tissue of larger trees is more vulnerable to embolism deserves further study. Taller trees are predisposed to greater hydraulic stress, from elevated atmospheric demand and longer hydraulic path lengths<sup>23</sup>. As the canopies are exposed to rainfall in the TFE, smaller trees could avoid hydraulic deterioration through leaf water uptake<sup>24–26</sup>, but this may not be sufficient to save the largest trees, which we hypothesize are forced to maintain their high growth rates until death to continually replace dysfunctional xylem.

Following decadal-scale soil moisture depletion, our results suggest that tropical rainforests will experience accelerating biomass loss and a likely transition to a lower statured, lower biomass forest state, due to substantially elevated mortality of the largest trees. This mortality is most likely triggered by hydraulic processes, which lead to hydraulic deterioration and subsequent, potentially rapid, limitations in carbon uptake<sup>21</sup>, instead of being caused directly by gradual carbon starvation. Under natural drought these forests may be under greater risk than from experimental drought, as severe soil moisture deficit is combined with low humidity and high air temperature, increasing hydraulic demand. Improved prediction of the sensitivity of tropical tree mortality to drought should therefore focus on improved model simulation of plant hydraulics and modelling environmental controls on growth<sup>22,27</sup>. Decadal-scale ecological data such as these are rare, but they are invaluable for testing and improving predictions from vegetation models over

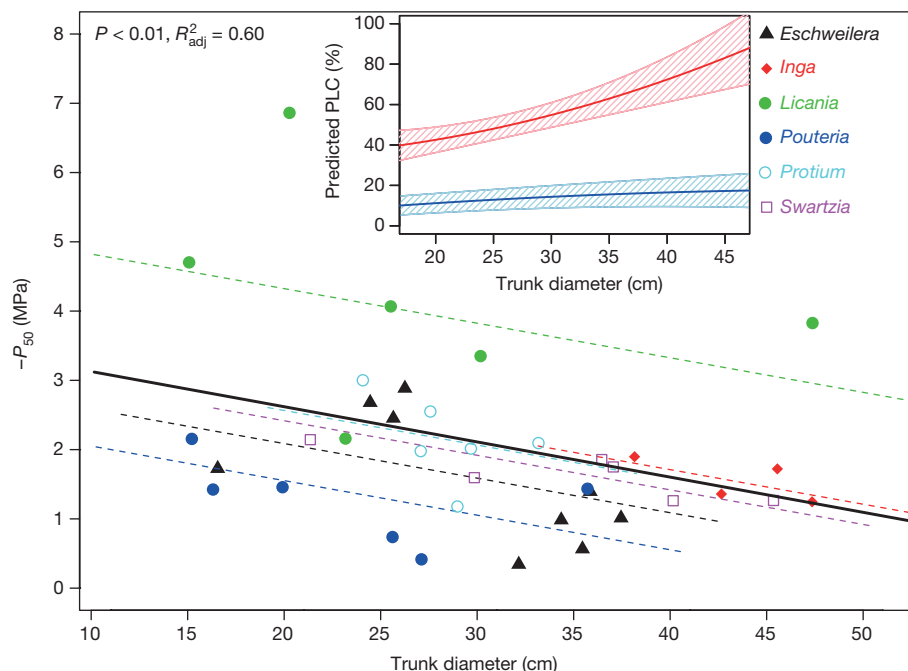


**Figure 4 | Xylem vulnerability to embolism and predicted loss of xylem hydraulic conductivity as a function of tree diameter (dbh).** A general linear model was employed to test for the effects of genus and tree dbh on the estimates of xylem  $P_{50}$  obtained for each species ( $n = 37$  trees in total). The dashed lines give the predicted regressions for each of the six genera, whereas the bold black line gives the overall mean regression line across all species (The adjusted  $R^2$  in the figure refers to the overall model, while the  $P$  value refers to the significance of tree dbh). The inset shows the predicted losses of hydraulic conductivity (PLC) as a function of tree size and mean midday  $\Psi_1$ . In the main graph, each genus is represented with a different symbol and/or colour, as detailed in the legend. In the inset, the bold lines represent the average prediction for the most vulnerable genus (red, *Pouteria*) and for the most resistant one (blue, *Licania*), with the shaded areas (pink, light blue) giving the respective 95% confidence intervals.

timescales that are relevant to climate change<sup>28</sup>. They also underpin the long-term environmental policy needed to manage the natural capital that is embedded in tropical rainforests.

**Online Content** Methods, along with any additional Extended Data display items and Source Data, are available in the online version of the paper; references unique to these sections appear only in the online paper.

**Received 12 May; accepted 2 September 2015.**

**Published online 23 November 2015.**

- Christensen, J. H. *et al.* in *Climate Change 2013: The Physical Science Basis. Contribution of Working Group I to the Fifth Assessment Report of the Intergovernmental Panel on Climate Change* (eds Stocker, T. F., Qin, D., Plattner, G.-K., Tignor, M., Allen, S. K. *et al.*) (Cambridge Univ. Press, 2013).
- Mora, C. *et al.* The projected timing of climate departure from recent variability. *Nature* **502**, 183–187 (2013).
- Reichstein, M. *et al.* Climate extremes and the carbon cycle. *Nature* **500**, 287–295 (2013).
- Boisier, J. P., Ciais, P., Ducharne, A. & Guimberteau, M. Projected strengthening of Amazonian dry season by constrained climate model simulations. *Nat. Clim. Chang.* **5**, 656–660 (2015).
- Hartmann, H., Adams, H. D., Anderegg, W. R. L., Jansen, S. & Zeppel, M. J. B. Research frontiers in drought-induced tree mortality: crossing scales and disciplines. *New Phytol.* **205**, 965–969 (2015).
- da Costa, A. C. L. *et al.* Effect of 7 yr of experimental drought on vegetation dynamics and biomass storage of an eastern Amazonian rainforest. *New Phytol.* **187**, 579–591 (2010).
- Doughty, C. E. *et al.* Drought impact on forest carbon dynamics and fluxes in Amazonia. *Nature* **519**, 78–82 (2015).
- O'Brien, M. J., Leuzinger, S., Philipson, C. D., Tay, J. & Hector, A. Drought survival of tropical tree seedlings enhanced by non-structural carbohydrate levels. *Nat. Clim. Chang.* **4**, 710–714 (2014).
- Nepstad, D. C., Tohver, I. M., Ray, D., Moutinho, P. & Cardinot, G. Mortality of large trees and lianas following experimental drought in an Amazon forest. *Ecology* **88**, 2259–2269 (2007).
- Phillips, O. L. *et al.* Drought sensitivity of the Amazon rainforest. *Science* **323**, 1344–1347 (2009).
- Brando, P. M. *et al.* Drought effects on litterfall, wood production and belowground carbon cycling in an Amazon forest: results of a throughfall reduction experiment. *Philos. Trans. R. Soc. B* **363**, 1839–1848 (2008).
- da Costa, A. C. L. *et al.* Ecosystem respiration and net primary productivity after 8–10 years of experimental through-fall reduction in an eastern Amazon forest. *Plant Ecol. Divers.* **7**, 7–24 (2014).
- Meir, P. *et al.* Threshold responses to soil moisture deficit by trees and soil in tropical rain forests: insights from field experiments. *Bioscience* **65**, 882–892 (2015).
- McDowell, N. G. *et al.* The interdependence of mechanisms underlying climate-driven vegetation mortality. *Trends Ecol. Evol.* **26**, 523–532 (2011).
- Thomas, H. Senescence, ageing and death of the whole plant. *New Phytol.* **197**, 696–711 (2013).
- Meir, P., Mencuccini, M. & Dewar, R. C. Drought-related tree mortality: addressing the gaps in understanding and prediction. *New Phytol.* **207**, 28–33 (2015).
- Anderegg, W. R. L. *et al.* Drought's legacy: multiyear hydraulic deterioration underlies widespread aspen forest die-off and portends increased future risk. *Glob. Chang. Biol.* **19**, 1188–1196 (2013).
- Rowland, L. *et al.* After more than a decade of soil moisture deficit, tropical rainforest trees maintain photosynthetic capacity, despite increased leaf respiration. *Glob. Chang. Biol.* (2015).
- Anderegg, W. R. *et al.* The roles of hydraulic and carbon stress in a widespread climate-induced forest die-off. *Proc. Natl Acad. Sci. USA* **109**, 233–237 (2012).
- Choat, B. *et al.* Global convergence in the vulnerability of forests to drought. *Nature* **491**, 752–755 (2012).
- Sala, A., Woodruff, D. R. & Meinzer, F. C. Carbon dynamics in trees: feast or famine? *Tree Physiol.* **32**, 764–775 (2012).
- Körner, C. Carbon limitation in trees. *J. Ecol.* **91**, 4–17 (2003).
- Mencuccini, M. *et al.* Size-mediated ageing reduces vigour in trees. *Ecol. Lett.* **8**, 1183–1190 (2005).
- Burkhardt, J., Basi, S., Pariyar, S. & Hunsche, M. Stomatal penetration by aqueous solutions – an update involving leaf surface particles. *New Phytol.* **196**, 774–787 (2012).
- Yates, D. J. & Hutley, L. B. Foliar uptake of water by wet leaves of *Sloanea woollsii*, an Australian subtropical rain-forest tree. *Aust. J. Bot.* **43**, 157–167 (1995).
- Eller, C. B., Lima, A. L. & Oliveira, R. S. Foliar uptake of fog water and transport belowground alleviates drought effects in the cloud forest tree species, *Drimys brasiliensis* (Winteraceae). *New Phytol.* **199**, 151–162 (2013).
- Faticchi, S., Leuzinger, S. & Körner, C. Moving beyond photosynthesis: from carbon source to sink-driven vegetation modeling. *New Phytol.* **201**, 1086–1095 (2014).
- Leuzinger, S. *et al.* Do global change experiments overestimate impacts on terrestrial ecosystems? *Trends Ecol. Evol.* **26**, 236–241 (2011).

**Acknowledgements** This work was supported by UK NERC grant NE/J011002/1 to P.M. and M.M., CNPQ grant 457914/2013-0/MCTI/CNPq/FNDCT/LBA/ESECAFLOR to A.C.L.D., and ARC grant FT110100457 to P.M. It was previously supported by NERC NER/A/S/2002/00487, NERC GR3/11706, EU FP5-Carbonsink and EU FP7-Amazalert to P.M. and J.G., and by grant support to Y.M. from NERC NE/D01025X/1 and the Gordon and Betty Moore Foundation. L.R., M.M. and P.M. would also like to acknowledge support from S. Sitth, Y. Salmon and B. Christoffersen. The authors would also like to thank three anonymous referees for their useful comments.

**Author Contributions** L.R., P.M., A.C.L.D. and M.M. designed and implemented the research. P.M. conceived and led the experiment and this study. L.R. led recent measurements; all authors contributed to data collection, led by A.C.L.D.; L.R. analysed the data with M.M., P.M., O.J.B. and A.M.P.; L.R. wrote the paper with P.M. and M.M., with contributions from all authors.

**Author Information** Reprints and permissions information is available at [www.nature.com/reprints](http://www.nature.com/reprints). The authors declare no competing financial interests. Readers are welcome to comment on the online version of the paper. Correspondence and requests for materials should be addressed to L.R. ([lucy.rowland@ed.ac.uk](mailto:lucy.rowland@ed.ac.uk)).

## METHODS

**Site.** The through-fall exclusion (TFE) experiment is located in the Caxiuana National Forest Reserve in the eastern Amazon (1° 43' S, 51° 27' W), ~400 km west of the nearest city, Belém, State of Pará, Brazil. The experiment is located in terra firma forest, on yellow oxisol soils which are 75–83% sand, 12–19% clay and 6–10% silt<sup>29</sup>. The site is 15 m above sea level, has a mean annual rainfall between 2,000–2,500 mm and a pronounced dry season between June and November<sup>2</sup>.

The experimental site has two 1-ha plots: the TFE, over which plastic panels and gutters have been placed at a height of 1–2 m, and which exclude 50% of the incident rainfall; and a corresponding control plot, <50 m from the TFE, on which there has been no manipulation of incident rainfall. The TFE was trenched to between 1–2 m to remove the effect of through-flow of soil water; and to control for any temporary damage to roots from the trenching, the control plot was also trenched to the same depth. The TFE treatment has been installed and running continuously since January 2002 to the present, except for a 1-week period in November 2002 (full removal), a month period during the dry season in November 2014 (sequential removal of all panel) and during 2004 (30% removal).

No statistical methods were used to predetermine sample size, the experiments were not randomized and the investigators were not blinded to allocation during experiments and outcome assessment.

**Soil moisture data.** In both the control and TFE plots there are soil access pits in which volumetric soil water content sensors (CS616, Campbell Scientific, Logan, USA) located at depths of 0, 0.5, 1, 2.5 and 4 m, monitor soil moisture every hour (see Fisher *et al.*<sup>30</sup> for full methodology). New data presented here are from March 2008–December 2014, averaged into monthly values. Due to equipment failure, some soil moisture data are missing for August and December 2013, for 2008 and 2010 on the control plot, and for November and December 2013 on the TFE plot. Volumetric soil water content was converted in to soil water potential ( $\Psi_s$ ) using the necessary van Genuchten parameters previously calculated by Fisher *et al.*<sup>31</sup> based on soil hydraulics measurements at this site.

**Biomass data.** Trees  $\geq 10$  cm diameter at breast height (dbh) on both the control and the TFE plots were tagged and identified to species level in September 2000. Diameters were measured on these trees at 1.3 m, unless buttress roots were present, in which case the measurement was made above the buttressing. Individuals on the plots were re-censused at varying intervals from January 2001, until November 2014. During each census the trees were also assessed to be either dead or alive. A tree was considered dead if leaflessness was accompanied by a persistent zero or negative stem increment, and/or the tree had snapped or fallen to the ground. Recruitment of new trees into the  $\geq 10$  cm dbh size class was enumerated in 2005, 2009 and 2014.

Trees in the 10 × 10 m subplots adjacent to the trenches were excluded from our biomass and growth rate analysis to eliminate possible effects of changes in mortality resulting from root damage<sup>2</sup>. Consequently, 369 trees on the control and 358 trees on the TFE, each in 0.64 ha were analysed and the biomass scaled to 1 ha. Following da Costa *et al.*<sup>6</sup> trees were grouped into small (10–20 cm dbh), medium (20–40 cm dbh) and large (>40 cm dbh) size classes.

Biomass was calculated using the Chave *et al.*<sup>32</sup> equation which uses diameter, wood density and environmental predictors. A mean and standard deviation of wood density for each tree was calculated from data in the global wood density database<sup>33,34</sup> and from Patiño *et al.*<sup>35</sup>. Multiple estimates of wood density at the species, genus and family level were used to calculate standard deviations on our wood density estimates. Of all the trees on both plots, 68% had values for wood density at species level, 18% at genus level and 3% at family level; 11% of trees were not identified and were given a plot level average wood density with an associated standard deviation. A standard error on our biomass estimations was calculated, which accounted for the error associated with wood density estimation and variations in commonly used allometric equations. Twelve calculations were used to calculate the error on our biomass values; these 12 biomass estimates were from combinations of four biomass equations: Chave *et al.*<sup>32</sup> and Chave *et al.*<sup>36</sup> both with and without height and three wood density estimates: mean wood density and mean wood density  $\pm$  one standard deviation. The allometric equations selected represent one of the most commonly used biomass equations for Amazonia<sup>36</sup> (with and without height as a predictor variable) and the most recent and most comprehensive biomass equations for our study area<sup>32</sup> (with and without height as a predictor variable). Measurements of height were not available and were calculated from an equation developed specifically for the region of the Amazon in which our plots are located<sup>37</sup>. Mortality rate was calculated according to da Costa *et al.*<sup>6</sup> and separately for trees of 10–20 cm dbh, 20–40 cm dbh and >40 cm dbh on the TFE and control plot.

**Seasonal growth data.** Dendrometers were installed at just above or below the point of dbh measurement on all trees  $\geq 10$  cm dbh<sup>38</sup>. Circumference measurements from the dendrometer bands were made monthly to tri-monthly from January 2005 to November 2014, with the exception of a six month gap from July

2007 and January 2013. Seasonal shrinkage was calculated by taking the average growth rate of 19 trees on the control and TFE plots which experienced no overall growth, but demonstrated a seasonal pattern of shrinkage and expansion. Tropical trees can experience net diameter shrinkage in the dry season, due to a lack of growth, accompanied by reduced water content of stem tissues, with subsequent swelling when tissues are rehydrated in the wet season<sup>39</sup>. An average pattern of shrinkage and expansion was therefore subtracted from all trees to ensure that dry season growth was not under-estimated and wet season growth over-estimated. Dendrometer increments were filtered to remove the growth spikes from measurement errors following Rowland *et al.*<sup>39</sup>. Subsequent to this procedure, gap-filling was done using linear interpolation<sup>39</sup>; on the control and TFE plot 16% and 17% of the data were gap-filled respectively. Growth rates per day calculated from the dendrometer measurements were averaged into three monthly periods to give continuous tri-monthly growth rates from 2005–2014. When trees in the 10 × 10 m subplots adjacent to the trenches, and trees with poor quality dendrometer measurements throughout the 10 year study period for growth were excluded, 316 and 310 trees on the control and TFE plot remained, respectively. All growth and mortality analyses were done using the R statistical package (version 3.1.2). Tests for significance were performed using Wilcoxon signed-rank test.

**Non-structural carbohydrate (NSC) analysis.** Using samples cut by a tree climber from fully sunlit branches, three leaves and a branch sample of ~8–10 mm diameter were taken from 20 trees on the control plot and 21 trees on the TFE plot in November 2013, March 2014 and June 2015. The numbers and species of the trees selected for analysis are shown in Extended Data Table 1. The selected trees were all >10 cm dbh and represented the most common genera existing on both plots<sup>2</sup>; samples were not taken from the external 10 × 10 m subplots to avoid any impacts of trenching. Samples of tree stem tissue from the same trees were taken with a 5 mm increment borer at breast height once in November 2013; this sampling was not repeated to avoid excessive damage incurred by repeated boring. We followed the enzymatic method proposed by Sevanto *et al.*<sup>40</sup> to analyse the NSC content. Here, NSC is defined as free, low-molecular-weight sugars (glucose, fructose and sucrose) and starch. Immediately after collection, samples were microwaved to stop enzymatic activity. After that, samples were oven-dried at 70 °C for 24–48 h and ground to fine powder. We prepared approximately 12 mg of plant material with 1.6 ml of distilled water for the analysis. We used amyloglucosidase from *Aspergillus niger* (Sigma-Aldrich) to digest total NSC to glucose, and invertase, glucose hexokinase kits (GHK) and phosphorus glucose (Sigma-Aldrich) to quantify the low molecular weight sugars. The concentration of free glucose was determined photometrically in a 96-well microplate spectrophotometer (BioTek, Epoch). NSC values are expressed as per cent of dry matter. For further method details, see Sevanto *et al.*<sup>40</sup>.

**Xylem vulnerability to cavitation (percentage loss of conductivity; PLC) and leaf water potential measurements.** Samples were cut from fully sunlit branches following the same protocol as above for NSC during late dry season (November 2013), and using the same sample trees as used for the NSC analysis (Extended Data Table 1), with the exception of branches of the genus *Manilkara*. To maintain a balance of number of genera and trees sampled, four additional trees were therefore sampled from the genus *Inga* in the TFE and control plots for both sets of analyses. One to three 1.0–1.5 m long branches per tree were cut and left to rehydrate overnight under a black plastic bag in a bucket of water. Maximum vessel length was determined for one branch out of a set of 5–6 branches for each species by injecting low pressure air at the branch base under water and progressively re-cutting the stem until bubbles emerged (maximum conduit length varied between 25 and 50 cm across samples)<sup>41</sup>. Axial slits were made in the branch segments selected for PLC analysis to increase the efficacy of the air injection. These partially debarked segments were mounted on a 4.6 cm long air injection apparatus. Water, filtered to 0.2  $\mu$ m, flowed gravimetrically through the sample. After 10 min of equilibration at low pressure (10 kPa), the sample was pressurised for 20 min. The pressure was increased in steps of 0.3 to 0.5 MPa, with each step followed by 10 min relaxation and flow measured at a constant background 100 kPa air pressure, until a residual flow lower than 5% of the initial flow was found. Five to ten measurements of water flux were taken at the distal end. The interval for each conductivity measurement ranged from 2 to 10 min depending on stem length, conductivity and pressure head employed (normally 3 kPa). Segment lengths, cross-sectional diameters and leaf areas of the leaves subtended by the measured segment were determined.

We employed a two-parameter Weibull function to model the changes in per cent loss of xylem hydraulic conductivity as a function of xylem pressure<sup>42</sup>. The two parameters represented  $P_{50}$  and slope of the conductivity-pressure curve. We estimated  $P_{50}$  and slope for all trees using tree as a random factor in a mixed-model analysis (nlme library<sup>43</sup>) in R (Version 3.0.2, R Core Team). We let  $P_{50}$  vary for each tree while keeping slope constant across trees to achieve convergence. We then employed these conditional estimates of  $P_{50}$  in a general linear model to test for the effects of plot, genus and dbh (Extended Data Table 2a).

We then confirmed the above results by running a second mixed-effect model, in which we accounted for random tree-by-tree variation and variance driven by phylogeny, by nesting individual trees within genera as the random component of the model and incorporating plot and dbh as fixed effects (Extended Data Table 2b). We tested whether tree diameter affected  $P_{50}$  by comparing the performance of the full model with the same model without the effect of dbh on  $P_{50}$  using a likelihood ratio test, and by conducting simultaneous hypothesis tests at the 95% significance level (library multcomp in R). For both analyses, distributional assumptions were tested by looking at plots of residuals for fixed and, if the case, random effects.

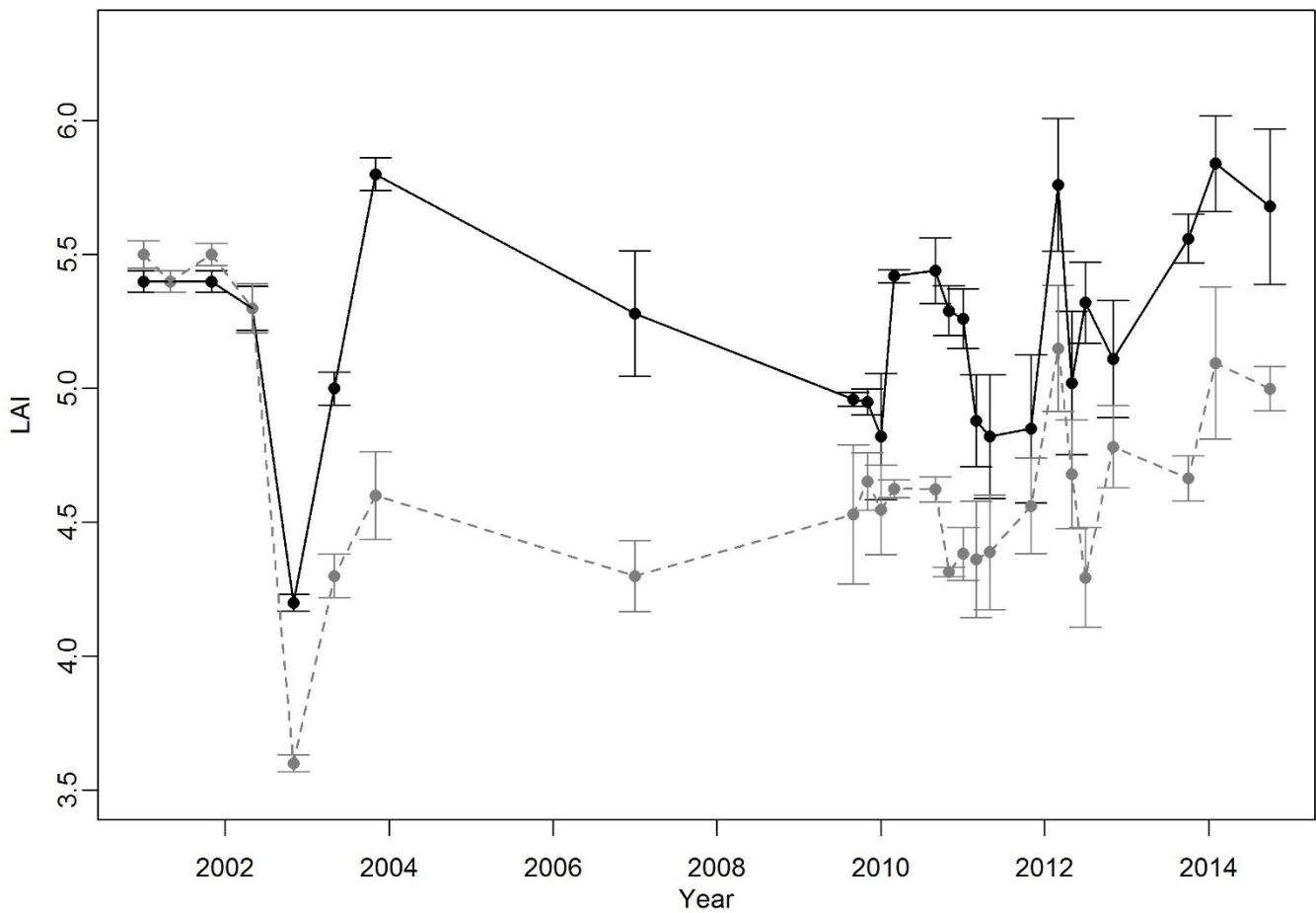
Leaf water potential  $\Psi_1$  was measured during two campaigns (one during the dry and one during the wet season, that is, October 2013 and May 2014, respectively). Two to four leaves were measured for each branch of each tree, following the same sampling protocol above for NSC and hydraulic measurements. During each campaign,  $\Psi_1$  measurements were conducted at pre-dawn (before 07:00) and at midday (between 11:30 and 13:00). Midday  $\Psi_1$  measurements of both campaigns were used in conjunction with the  $P_{50}$  and slope values determined for each genus to estimate percent loss of hydraulic conductivity (PLC), assuming xylem water potential to be equal to measured leaf water potential<sup>20</sup>. We acknowledge that this may overestimate PLC; however in counterpoint, only one seasonal campaign could be conducted and so the minimum of leaf  $\Psi_1$  for that year was thus likely to have been underestimated because fuller sampling through the dry season was impractical. In addition, earlier (2003) studies in the same experiment<sup>44</sup> reported minimum values of stem xylem water potentials of around  $-1.6$  MPa, across control and TFE plots, suggesting that xylem values substantially more negative than those assumed here can be experienced.

**Herbivory.** All leaf material from  $25 \times 1 \text{ m}^2$  litter-traps on the control and TFE was collected 13 times from 2010–2014 at 3–6 month intervals, with one eight month interval in 2011. Each collection of leaf material represented two weeks of litter-fall in the forest. The 7,121 leaves collected from all 25 per plot litter-traps over the study period were scanned and the images were analysed according to Metcalfe *et al.*<sup>45</sup> to calculate the percent leaf area lost to herbivore attack on the control and TFE.

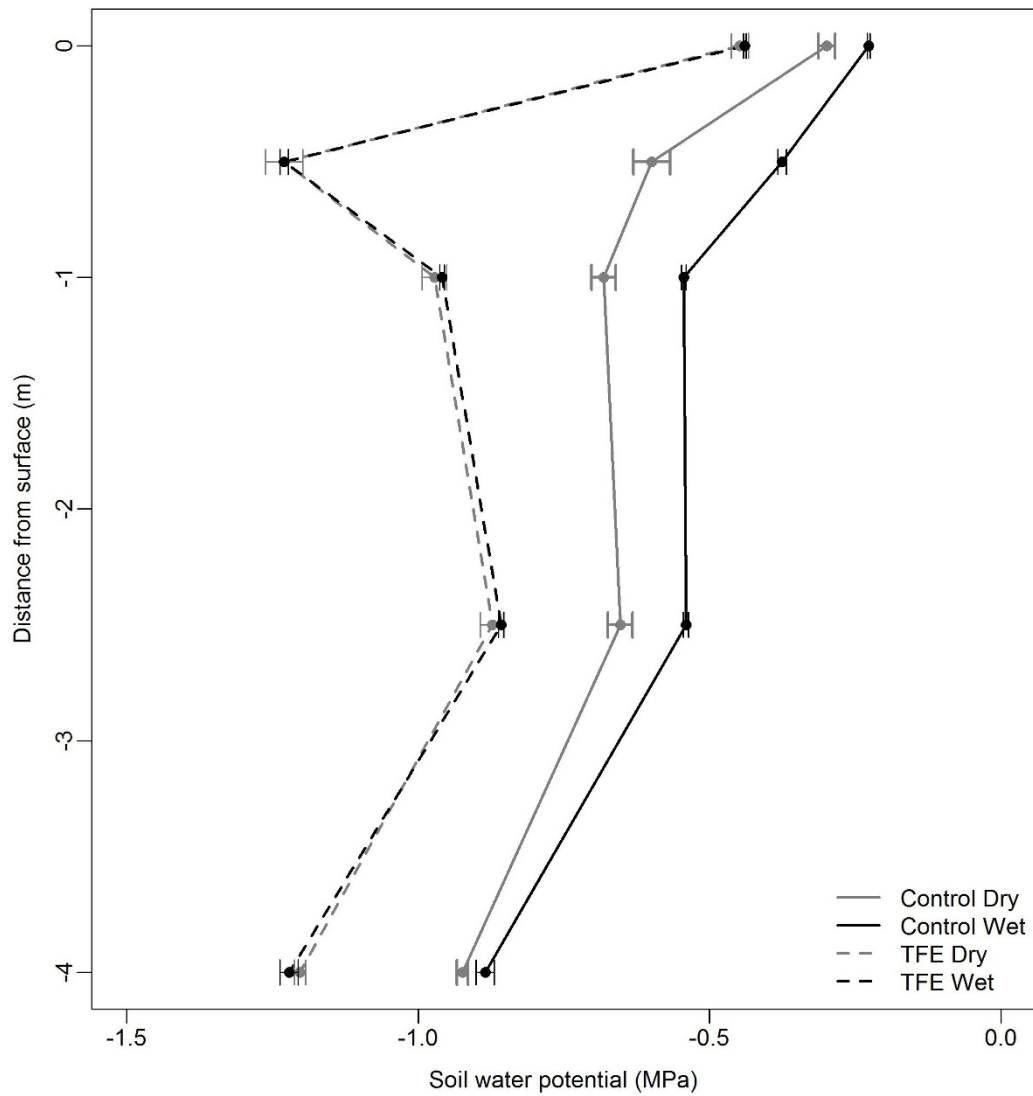
**LAI measurements.** LAI values from 2001 to 2007 are taken from Fig. 1f in Metcalfe *et al.*<sup>38</sup>. For 2009–2014 LAI was measured at the same 25 permanent points<sup>38</sup> on a grid throughout the control and TFE plot. Measurements were made using hemispherical photos taken every 3–6 months from 2009–2014. Photos were taken before sunrise ( $\sim 6:00$ ) from a height of 1.5 m on the control plot and 2 m (above the TFE structure) on the TFE plot. The 25 photos per plot were analysed

together using the CAN\_EYE software (INRA, Avignon, France). Standard errors were calculated using three different estimates of LAI given by the CAN\_EYE software.

29. Ruivo, M. L. P. & Cunha, E. C. in *Ecosystems and sustainable development IV* (eds Tiezzi, E., Brebbia, C. A. & Uso, J.-L.) Vol. 2, 1113–1121 (WIT Press, 2003).
30. Fisher, R. A. *et al.* The response of an Eastern Amazonian rain forest to drought stress: results and modelling analyses from a throughfall exclusion experiment. *Glob. Chang. Biol.* **13**, 2361–2378 (2007).
31. Fisher, R. A., Williams, M., Ruivo, M. D., de Costa, A. L. & Meira, P. Evaluating climatic and soil water controls on evapotranspiration at two Amazonian rainforest sites. *Agric. For. Meteorol.* **148**, 850–861 (2008).
32. Chave, J. *et al.* Improved allometric models to estimate the aboveground biomass of tropical trees. *Glob. Chang. Biol.* **20**, 3177–3190 (2014).
33. Chave, J. *et al.* Towards a worldwide wood economics spectrum. *Ecol. Lett.* **12**, 351–366 (2009).
34. Zanne, A. E. *et al.* Data from: Towards a worldwide wood economics spectrum. Dryad Digital Repository. <http://dx.doi.org/10.5061/dryad.234> (2009).
35. Patiño, S. *et al.* Branch xylem density variations across the Amazon Basin. *Biogeosciences* **6**, 545–568 (2009).
36. Chave, J. *et al.* Tree allometry and improved estimation of carbon stocks and balance in tropical forests. *Oecologia* **145**, 87–99 (2005).
37. Feldpausch, T. R. *et al.* Tree height integrated into pantropical forest biomass estimates. *Biogeosciences* **9**, 3381–3403 (2012).
38. Metcalfe, D. B. *et al.* Shifts in plant respiration and carbon use efficiency at a large-scale drought experiment in the eastern Amazon. *New Phytol.* **187**, 608–621 (2010).
39. Rowland, L. *et al.* The sensitivity of wood production to seasonal and interannual variations in climate in a lowland Amazonian rainforest. *Oecologia* **174**, 295–306 (2014).
40. Sevanto, S., McDowell, N. G., Dickman, L. T., Pangle, R. & Pockman, W. T. How do trees die? A test of the hydraulic failure and carbon starvation hypotheses. *Plant Cell Environ.* **37**, 153–161 (2014).
41. Ennajeh, M., Simões, F., Khemira, H. & Cochard, H. How reliable is the double-ended pressure sleeve technique for assessing xylem vulnerability to cavitation in woody angiosperms? *Physiol. Plant.* **142**, 205–210 (2011).
42. Neufeld, H. S. *et al.* Genotypic variability in vulnerability of leaf xylem to cavitation in water-stressed and well-irrigated sugarcane. *Plant Physiol.* **100**, 1020–1028 (1992).
43. Pinheiro, J. C. & Bates, D. M. *Mixed-Effects Models in S and S-PLUS* (Springer, 2000).
44. Fisher, R. A., Williams, M., Do Vale, R. L., Da Costa, A. L. & Meir, P. Evidence from Amazonian forests is consistent with isohydric control of leaf water potential. *Plant Cell Environ.* **29**, 151–165 (2006).
45. Metcalfe, D. B. *et al.* Herbivory makes major contributions to ecosystem carbon and nutrient cycling in tropical forests. *Ecol. Lett.* **17**, 324–332 (2014).



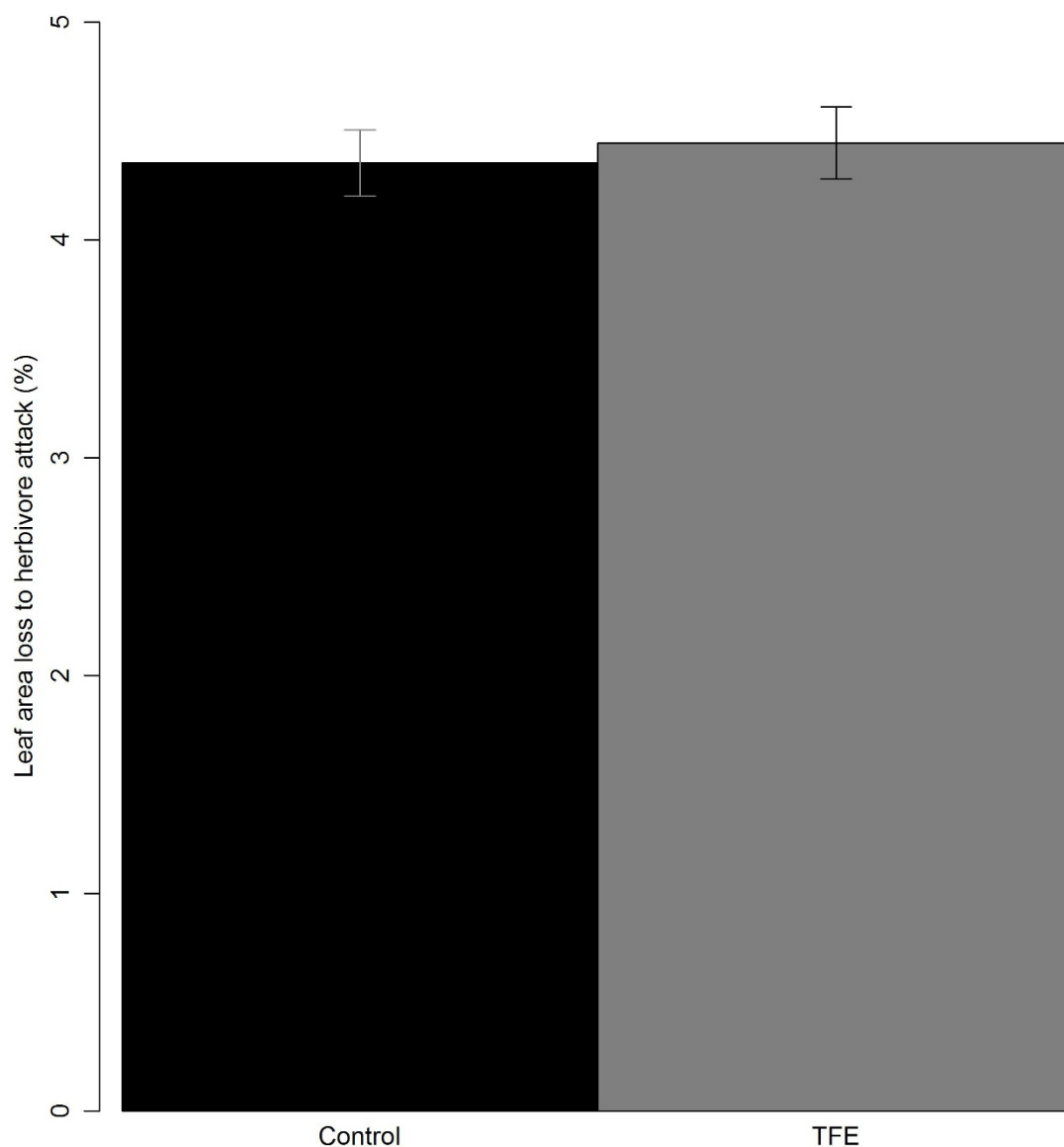
**Extended Data Figure 1 | Leaf area index change.** Leaf area index (LAI; ratio of leaf area to ground area) for the period of 2001–2014 on the control (black, solid) and TFE (grey, dashed) plots. Error bars show the s.e.m. associated with LAI calculation, which is derived from  $n = 25$  photos per control and TFE plot (see Methods).



**Extended Data Figure 2 | Seasonal soil water potential.** Average soil water potential ( $-$ MPa) in the control and TFE during dry season (July–December, control  $n = 34$  months, TFE  $n = 40$  months) and wet season (January–June control  $n = 34$  months, TFE  $n = 40$  months), calculated from monthly average volumetric soil moisture content data,

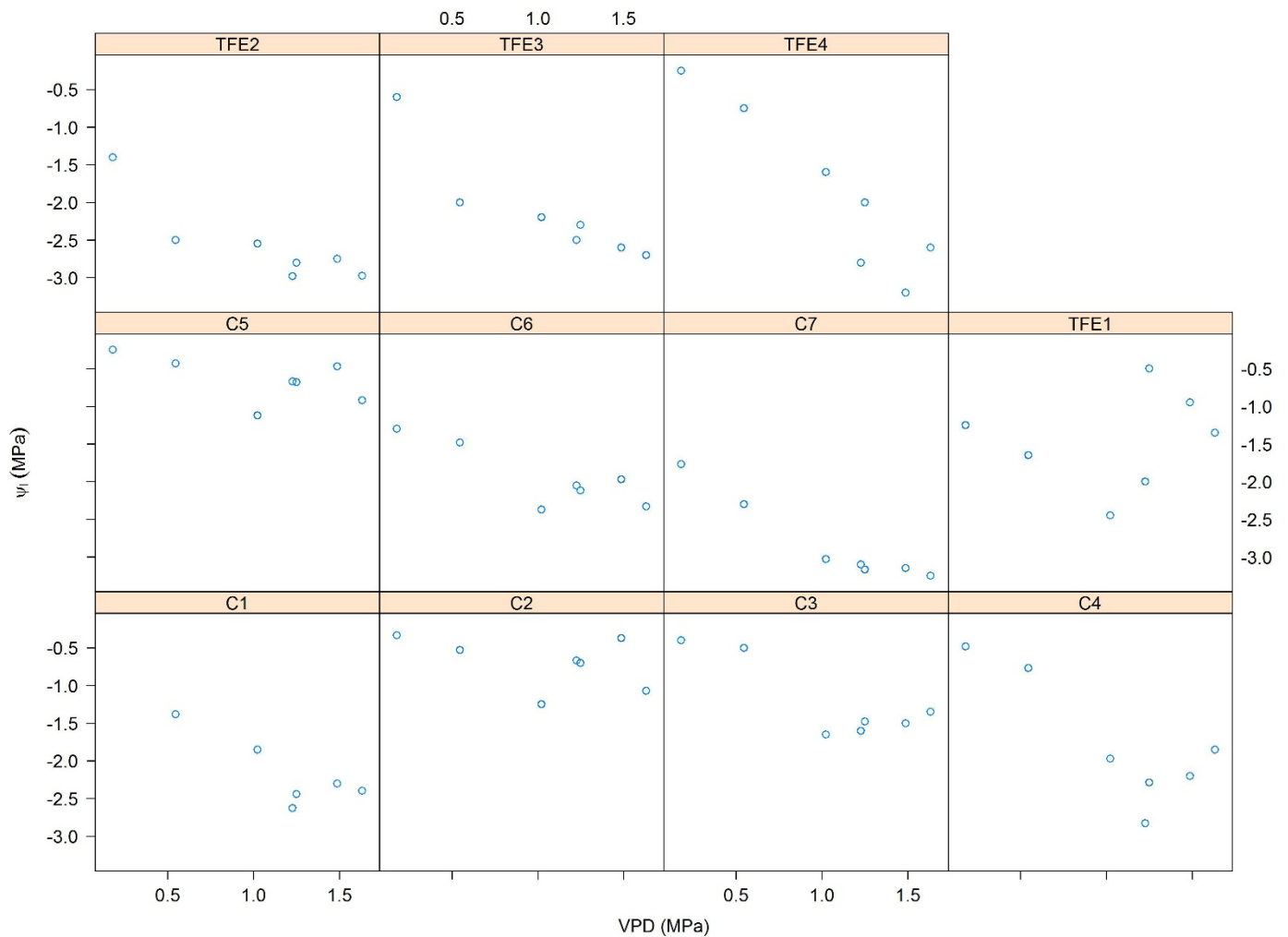
collected from 2008–2014, using sensors installed 0, 0.5, 1, 2.5 and 4 m below the surface and the necessary van Genuchten parameters previously calculated from soil hydraulics measurements at this site (see Methods). Error bars show s.e.m.





**Extended Data Figure 3 | Leaf herbivory comparison.** Average percentage loss of leaf area from herbivore attack calculated from leaves collected in litter-traps on the control ( $n = 3,297$ ) and TFE plot ( $n = 3,824$ ) from 2010–2014. Error bars show s.e.m and no significant differences were found significant with a  $P < 0.05$  using the Wilcoxon test. A separate

analysis of herbivore attack on 13,694 top-canopy living leaves from branches of the 41 trees used for the  $P_{50}$  analysis support these results, also showing no significant differences in percentage herbivory between the control and the TFE (data not shown).



**Extended Data Figure 4 | Diurnal patterns of  $\Psi_l$ .** Diurnal  $\Psi_l$  measured every 2 h from 6:00 until 18:00 in dry season on trees accessible from the walk up tower. Each box shows the diurnal  $\Psi_l$  against diurnal air vapour pressure deficit (VPD) from one of seven trees accessible on the control (C), or one of four trees accessible on the TFE. Note that a majority of

trees demonstrate an inversely correlated (negative) relationship with VPD. Combined separately for each plot, a significant negative linear relationship is observed between  $\Psi_l$  and VPD on the control ( $R^2 = 0.18$ ,  $P = 0.002$ ) and even more strongly on the TFE ( $R^2 = 0.33$ ,  $P = 0.001$ ).

Extended Data Table 1 | NSC and  $P_{50}$  sample trees

Genus	Species	Control			TFE		
		Number	dbh (cm)	$P_{50}$ (MPa)	Number	dbh (cm)	$P_{50}$ (MPa)
<i>Eschweilera</i>	<i>grandiflora</i>	1	36.5	0.6	1	16.8	
		2	34.5	1.0	2	16.7	1.7
		3			3	24.6	2.7
	<i>coriacea</i>	3	37.6	1.0	4	26.4	2.9
					5	32.3	0.3
					6	36.0	1.4
<i>Licania</i>	<i>pedicellata</i>	4	17.8				
		5	25.8	2.5			
	<i>membranacea</i>	6	20.5	6.9	7	15.5	4.7
		7	23.4	2.2	8	25.6	4.1
<i>Manilkara</i>	<i>octandra bidentata</i>				9	47.6	3.8
		8	30.4	3.3			
		9	32.1		10	29.3	
		10	32.5		11	36.7	
		11	48.4		12	56.1	
<i>Pouteria</i>	<i>anomala</i>	12	15.4	2.2	13	20.1	1.5
		13	16.4	1.4	14	25.8	0.7
		14	35.9	1.4	15	27.3	0.4
<i>Protium</i>	<i>tenuifolium</i>	15	24.3	2.0	16	27.8	2.5
		16	29.9	3.0	17	29.2	1.2
		17	33.4	2.1			
		<i>paniculatum</i>			18	37.3	2.0
<i>Swartzia</i>	<i>racemosa</i>	18	30.0	1.6	19	21.5	2.1
		19	37.2	1.3	20	36.2	1.9
		20	45.5	1.7	21	40.3	1.3
<i>Inga</i>	<i>alba</i>	21	38.3	1.9	22	45.7	1.7
		22	42.8	1.4	23	47.5	1.2

The genus, species and number of trees >10 cm dbh sampled for NSC and  $P_{50}$  from the central 0.64 ha area of each of the control and TFE plots, and their  $P_{50}$  value. The dbh (in cm) of the sample trees is shown in brackets. Where possible, trees from the most common species within the most common genera were sampled; when this was not possible a second species within the same genus was sampled. The genera shown here represent seven of the most abundant genera found across both plots<sup>2</sup>. The samples from the genus *Inga* were only employed for leaf water potential and  $P_{50}$  measurements to replace *Manilkara* samples from which  $P_{50}$  data were unobtainable.

Extended Data Table 2 | Analysis of the effect of tree dbh on xylem  $P_{50}$ 

	Degrees of freedom	Sum Squares	Mean Square	F value	Probability	
<b>Tree dbh</b>	1	6.139	6.1390	9.1974	0.0051	**
<b>Plot</b>	1	0.095	0.0950	0.1423	0.7087	ns
<b>Genus</b>	5	32.917	6.5834	9.8632	1.4 e-5	***
<b>Residuals</b>	29	19.357	0.6675			

Model covariates	Degrees of freedom	AIC	Log-likelihood	Likelihood ratio	P-value
<b>without tree dbh</b>	6	2793	-1393	28.2	<0.0001
<b>with tree dbh</b>	4	2769	-1378		

Top, analysis of variance table from the general linear model testing for the effects of plot, genus and dbh on xylem  $P_{50}$ . Bottom, difference in maximum likelihood for the mixed-model with and without tree size as a predictor of xylem  $P_{50}$  (see Methods).

The table shows the main parameters and the significance level of the  $\chi^2$  test of the likelihood ratio test. ns, not significant; \*\*, highly significant; \*\*\*, very highly significant.

Extended Data Table 3 | Individual tree mortality by genus

control plot			TFE plot		
Genus	No.	Year dead	Genus	No.	Year dead
<i>Aspidosperma</i>	1	2007	<i>Abuta</i>	1	2014
<i>Buchenavia</i>	1	2003	<i>Bauhinia</i>	1	2009
<i>Couratari</i>	3	2013,2013,2014	<i>Brosimum</i>	1	2005
<i>Duguetia</i>	2	2004,2005	<i>Chimarrhis</i>	1	2014
<i>Eschweilera</i>	3	2009, 2013, 2013	<i>Couepia</i>	1	2005
<i>Eugenia</i>	1	2001	<i>Dendrobangia</i>	2	2005,2005
<i>Franchetella</i>	1	2014	<i>Derris</i>	1	2005
<i>Guatteria</i>	2	2005,2005	<i>Doliocarpus</i>	1	2009
<i>Helicostylis</i>	1	2007	<i>Erismia</i>	1	2006
<i>Inga</i>	2	2009,2013	<i>Eschweilera</i>	3	2006,2007,2007
<i>Iryanthera</i>	1	2013	<i>Forsteronia</i>	1	2009
<i>Licania</i>	4	2002,2008,2013,2013	<i>Goupia</i>	4	2002,2004,2013,2014
<i>Micropholis</i>	1	2002	<i>Guatteria</i>	2	2008,2009
<i>Minquartia</i>	2	2003,2004	<i>Hirtella</i>	1	2009
<i>NI</i>	4	2001,2002,2013,2013	<i>Inga</i>	4	2005,2008,2008,2014
<i>Parkia</i>	1	2014	<i>Iryanthera</i>	1	2014
<i>Pouteria</i>	4	2003,2007,2009,2010	<i>Lecythis</i>	5	2004,2009,2009,2013,2013
<i>Protium</i>	4	2005,2009,2014,2014	<i>Licania</i>	2	2008, 2009
<i>Rinoria</i>	4	2004,2009,2013,2014	<i>Machaerium</i>	1	2003
<i>Sclerolobium</i>	1	2005	<i>Manilkara</i>	4	2004,2004,2008,2014
<i>Stachyarrhena</i>	1	2014	<i>Marmaroxylon</i>	1	2001
<i>Stryphnodendron</i>	1	2006	<i>Mezilaurus</i>	1	2008
<i>Swartzia</i>	4	2002,2003,2007,2014	<i>Micropholis</i>	4	2003,2005,2007,2009
<i>Tapura</i>	1	2014	<i>Minquartia</i>	1	2009
<i>Tetragastris</i>	2	2006,2013	<i>Naucleopsis</i>	1	2002,2007,2014
<i>Vantanea</i>	1	2003	<i>Newtonia</i>	1	2009
<i>Virola</i>	1	2006	<i>NI</i>	2	2002,2013
<i>Vouacapoua</i>	2	2013,2014	<i>Ocotea</i>	4	2002,2008,2009,2013
			<i>Oenocarpus</i>	1	2008
			<i>Ormosia</i>	2	2001, 2009
			<i>Ouratea</i>	4	2006,2007,2009,2014
			<i>Pouteria</i>	6	2005,2005,2007, 2009,2013,2014
			<i>Pradosia</i>	1	2005
			<i>Protium</i>	5	2005,2007,2007,2009,2009
			<i>Pseudolmedia</i>	2	2002, 2006
			<i>Quararibea</i>	1	2009
			<i>Sclerolobium</i>	1	2014
			<i>Stachyarrhena</i>	3	2007,2013,2014
			<i>Swartzia</i>	1	2004
			<i>Symphonia</i>	1	2014
			<i>Tetragastris</i>	1	2006, 2013, 2014
			<i>Xylopia</i>	5	2002,2004,2005,2014,2014

The number (No.) of dead trees per genus and the year of death (Year dead) for trees on the control and the TFE, excluding the outer subplots (see Methods). Trees not identified to genus are shown as *NI*.